J. KSIAM Vol.17, No.2, 67–85, 2013 http://dx.doi.org/10.12941/jksiam.2013.17.067

PATCHWISE REPRODUCING POLYNOMIAL PARTICLE METHOD FOR THICK PLATES: BENDING, FREE VIBRATION, AND BUCKLING

HYUNJU KIM[1†] AND BONGSOO JANG[2]

[1]DEPARTMENT OF MATHEMATICS AND STATISTICS, UNIVERSITY OF NORTH CAROLINA AT CHARLOTTE, CHARLOTTE, NC 28223, USA
E-mail address: hkim507@gmail.com

[2]SCHOOL OF TECHNOLOGY MANAGEMENT, ULSAN NATIONAL INSTITUTE OF SCIENCE AND TECHNOLOGY (UNIST), ULSAN METROPOLITAN CITY 689-798, REPUBLIC OF KOREA
E-mail address: bsjang@unist.ac.kr

ABSTRACT. Reproducing Polynomial Particle Method (RPPM) is one of meshless methods that use meshes minimally or do not use meshes at all. In this paper, the RPPM is employed for free vibration analysis of shear-deformable plates of the first order shear deformation model (FSDT), called Reissner-Mindlin plate. For numerical implementation, we use flat-top partition of unity functions, introduced by Oh et al, and patchwise RPPM in which approximation functions have high order polynomial reproducing property and the Kronecker delta property. Also, we demonstrate that our method is highly effective than other existing results for various aspect ratios and boundary conditions.

1. INTRODUCTION

The classical plate theories (CPT) based on the Kirchhoff hypothesis, are often used for thin plates. But these classical theories are inadequate to predict the gross response characteristics of moderately thick laminated composite plates as well as plates with high anisotropy. Usually in thicker plates, the vibration solutions are unconservatively high. The inaccuracy is caused by ignoring the transverse shear and normal strains in the plates. Thus, many shear deformation plate theories were developed to improve the analysis of the vibration of plates, and this had led to more accurate results. The first order shear deformation plate theory (FSDT) extends the kinematics of the CPT, in which transverse normal and shear stresses are neglected by relaxing the normality restriction and allowing for arbitrary but constant rotation of transverse

Received by the editors December 14 2012; Accepted February 19 2013.
2000 *Mathematics Subject Classification.* 74S06.
Key words and phrases. Meshfree methods; partition of unity function with flat-top; reproducing polynomial particle shape functions; Reissner-Mindlin plate theory.
The second author's work is supported by Basic Science Research Program Through the National Research Foundation of Korea(NRF) funded by the Ministry of Education, Science and Technology (No. 2010-0013297).
† Corresponding author.

normals. Numerous papers and books have been published on the vibration analysis of plates using various plate theories [23, 30, 39, 44].

The buckling analysis of plates is another class of eigenvalue problem. As is well known, a plate may lose its ability to withstand the external loadings, when the in-plane strain reaches a critical level. This phenomenon is the buckling of the plate, and the corresponding critical load at which the plate starts to become unstable, is termed the buckling load.

To analyze the buckling behavior of a thin plate, the CPT is often used. However, similar to the vibration of plates, when the thickness of the plate increases, the transverse shear-deformation effects will significantly influence the results of the buckling analysis. Thus the CPT is not applicable, and FSDTs [40, 19] are often resorted to analyze the buckling behavior instead of the CPT. Furthermore, the use of CPT may result in a different buckling mode shape compared with those of other plate theories, such as 3D elasticity theory, FSDT or higher order shear-deformation theory (HSDT).

Many methodologies have been implemented for various plate buckling and free vibration problems. These methods include analytical and numerical techniques, such as the Ritz method [8, 18], differential quadrature method [5, 45], finite strip methods [10], the finite element method [17, 41], and meshfree methods [22, 24] etc.

Meshless methods [1, 2, 3, 4, 20, 24, 42, 43] have several advantages over the conventional finite element method [6, 7, 31]. Their flexibility and wide applicability have gained attention from scientists and engineers to dynamic research areas [13, 14, 15]. Meshless methods employ flexible smooth base functions and use no mesh or use minimal background meshes. Actually, meshless methods have been referred to as meshfree methods [1, 2, 3], Reproducing Kernel Particle Methods(RKPM) [16, 20, 26, 27, 28], Reproducing Kernel Element Methods (RKEM) [20, 21, 25], Generalized Finite Element Methods (GFEM) (Partition or Unity Finite Element Methods (PUFEM)) [29, 42, 43], $h-p$ Cloud Method [11] and Element Free Galerkin Method (EFGM) [1].

Although these approaches are applicable in solving many difficult science and engineering problems, they have some difficulties: (1) The popular partitions of unity, an essential ingredient of GFEM, is complicated (such as Shepard type PU functions) or leads to singular stiffness matrix (when linear finite element bases functions are used as PU functions); (2) These popular PU functions have limited regularities; (3) When enriched local approximation functions are introduced, the integrations for these functions require much longer computing times; (4) These popular PU functions do not satisfy the Kronecker delta property except for hat functions. They have difficulties in implementing non-homogeneous essential boundary conditions.

To overcome these difficulties, encountered in meshless methods, Oh et al introduced three closed- form partition of unity (PU) functions that have flat-top: (1) Convolution partition of unity [36] for any partition of a given domain; Using convolution partition of unity, Oh et al. introduced several meshless methods that are called patchwise RPPM, adaptive RPPM, and RSPM (Reproducing Singularity Particle Method) in [32, 35, 36, 38]. Note that RPPM is similar to RKPM [2, 16, 20, 21, 25, 26, 27, 28]. (2) Almost everywhere partition of unity [33] that satisfies partition of unity property except at corner points. (3) Generalized product

partition of unity [34]. Using PU functions with flat-top gives relatively small matrix condition numbers.

In this paper, we apply PU function with flat-top to construct smooth local approximation functions that have the reproducing polynomial property and the Kronecker delta property.

In section 2, we introduce definitions and terminologies that are used in this paper, and briefly review the partition of unity functions with flat-top. In section 3, the variational formulation of Reissner-Mindlin plate for free vibration and buckling is described. In section 4, effectiveness of the reproducing polynomial particle method (RPPM) is demonstrated with various aspect ratio of plates. Finally, the concluding remarks are given in section 5.

2. Closed-form Partition of Unity with flat-top

Let $\bar{\Omega}$ is the closure of $\Omega \subset \mathbb{R}^d$. We define the vector space $\mathcal{C}(\bar{\Omega})$ to consist of all those functions $\varphi \in \mathcal{C}^m(\Omega)$ for which $D^\alpha\varphi(= \partial^{\alpha_1}\partial^{\alpha_2}\cdots\partial^{\alpha_d}\varphi)$ is bounded and uniformly continuous on Ω for $|\alpha| = \alpha_1 + \cdots + \alpha_d \leq m$. In the following, a function $\varphi \in \mathcal{C}^m(\Omega)$ is said to be a $\mathcal{C}^m$-function. If Ψ is a function defined on Ω, we define the *support* of Ψ as

$$\mathrm{supp}\Psi = \overline{\{x \in \Omega | \Psi(x) \neq 0\}}.$$

A family $\{U_k : k \in \mathcal{D}\}$ of open subsets of $\mathbb{R}^d$ is said to be *a point finite open covering* of $\Omega \subseteq \mathbb{R}^d$ if there is an integer M such that any $x \in \Omega$ lies in at most M of the open sets U_k and $\Omega \subseteq \bigcup_k U_k$.

For a point finite open covering $\{U_k : k \in \mathcal{D}\}$ of a domain Ω, suppose there is a family $\{\varphi_k : k \in \mathcal{D}\}$ of Lipschitz functions on Ω satisfying the following conditions:

(1) For $k \in \mathcal{D}$, $0 \leq \varphi_k(x) \leq 1, \quad x \in \mathbb{R}^d$.
(2) The support of φ_k is contained in $\overline{U}_k$, for each $k \in \mathcal{D}$.
(3) $\sum_{k\in\mathcal{D}} \varphi_k(x) = 1$ for each $x \in \Omega$.

Then $\{\varphi_k : k \in \mathcal{D}\}$ is called *a partition of unity (PU)* subordinate to the covering $\{U_k : k \in \Lambda\}$. The covering sets $\{U_k\}$ are called *patches*.

By *almost everywhere partition of unity*, we mean $\{\varphi_k : k \in \mathcal{D}\}$ such that the condition 3 of a partition of unity is not satisfied only at finitely many points (2D) or lines (3D) on a part of the boundary.

Let $Q = \mathrm{supp}(\varphi)$. Then $Q^{flt} = \{x \in Q : \varphi(x) = 1\}$ and $Q^{n\text{-}flt} = \overline{\{x \in Q : 0 < |\varphi(x)| < 1\}}$ are called the *flat-top* part and the *non flat-top* part of Q, respectively. The function φ is said to be *a function with flat-top* if the interior of Q^{flt} is non-void. Moreover, $\{\varphi_k : k \in \mathcal{D}\}$ is called a *partition of unity with flat-top* whenever it is partition of unity and φ_k is a function with flat-top for each $k \in \mathcal{D}$.

Notice that if $f_1, \cdots, f_n$ are linearly independent on $Q^{flt} \neq \varnothing$, the product functions, $\varphi \cdot f_1, \cdots, \varphi \cdot f_n$, are also linearly independent on Q. However, if $Q^{flt} = \varnothing$, the product functions, $\varphi \cdot f_1, \cdots, \varphi \cdot f_n$, could be linearly dependent. The hat functions of the conventional finite element are PU functions without flat-top.

Let Λ be a finite index set and Ω denotes a bounded domain in $\mathbb{R}^d$. Let $\{x_j : j \in \Lambda\}$ be a set of a finite number of uniformly or non-uniformly spaced points in $\mathbb{R}^d$, that are called *particles*.

The reproducing polynomial particle method (RPPM) is a Galerkin approximation method associated with use of reproducing polynomial shape functions for local approximation functions. Referring to [37], we introduce the following two definitions.

Definition 2.1. *(Reproducing Polynomial Property)*
Let Ω be a domain in $\mathbb{R}^n$, and $k \geq 0$ be an integer. The particle shape function ψ_j corresponding to the particle $x_j \in \mathbb{R}^n$, $j \in \Lambda$, is called reproducing polynomial of order k on Ω (or simply, reproducing of order k on Ω) if for any $x \in \Omega$,

$$p(x) = \sum_{j \in \Lambda} p(x_j)\psi_j(x) \text{for any } p \in P_k(\Omega),$$

where $P_k(\Omega)$ is the space of all polynomials of degree up to k on Ω and Λ is an index set.

Definition 2.2. *(RPP Shape Function) Let $k \geq 0$ be an integer. Let X be a set of particles in $\mathbb{R}^n$ with the index set Λ. Then the function ψ_j associated with the particles x_j, $j \in \Lambda$, are called reproducing polynomial particle (RPP) shape functions with the reproducing property of order k (or simply, of reproducing order k) if and only if they are piecewise polynomials and satisfy the following:*

For any $x \in \Omega \subseteq \mathbb{R}^n$,

$$\sum_{j \in \Lambda} (x - x_j)^\beta \psi_j(x) = \delta_{|\beta|,0}, \quad \text{for all } \beta \leq k. \tag{2.1}$$

Note that we assume that the RPP shape functions are translation invariant on the uniformly distributed particles, unless stated otherwise.

The piecewise polynomial RPP shape functions have several features different from Reproducing Kernel Particle (RKP) shape functions. The piecewise polynomial RPP shape functions are constructed by solving the system (2.1) without using window function, whereas the RKP shape functions are constructed by solving the system

$$\psi_j(x) = w(x - x_j) \sum_{0 \leq |\alpha| \leq k} (x - x_j)^\alpha b_\alpha(x),$$

with respect to a specific window function $w(x)$. Therefore, the RKP shape functions are not piecewise polynomials in general. It means that the RPP shape functions have no relevance to any specific window functions. However, both RPP and RKP shape functions are constructed to have the polynomial reproducing property.

Although there are particles on the boundaries because of the selected window function, the resulting RKP shape functions are not piecewise polynomial, so that can not be piecewise polynomial shape functions. Also, the support of the piecewise polynomial RPP shape functions are bounded by the particles, whereas the support of the RKP shape functions are bounded by points between two particles. Moreover, RKP shape functions do not satisfy the Kronecker delta property, and hence they have difficulties in dealing with Dirichlet boundary conditions. Whereas RPP shape functions satisfy the Kronecker delta property. Hence we do not need

additional numerical scheme to impose essential boundary conditions. (See [37, 38] for more details.)

2.1. **Partition of Unity with flat-top in one-dimension.** First, we define one-dimensional PU functions without flat-top, and then we modify the PU functions to have flat-top.

For any positive integer n, $\mathcal{C}^{n-1}$- piecewise polynomial basic PU functions are constructed as follows: For integer $n \geq 1$, we define a piecewise polynomial function by

$$\varphi_{g_n}^{(pp)}(x) = \begin{cases} \varphi_{g_n}^{L}(x) := (1+x)^n g_n(x) & \text{if} \quad x \in [-1, 0], \\ \varphi_{g_n}^{R}(x) := (1-x)^n g_n(-x) & \text{if} \quad x \in [0, 1], \\ 0 & \text{if} \quad |x| \geq 1, \end{cases}$$

where $g_n(x) = a_0^{(n)} + a_1^{(n)}(-x) + a_2^{(n)}(-x)^2 + \cdots + a_{n-1}^{(n)}(-x)^{n-1}$ whose coefficients are inductively constructed by the following recursion formula:

$$a_k^{(n)} = \begin{cases} 1 & \text{if} \quad k = 0, \\ \sum_{j=0}^{k} a_j^{(n-1)} & \text{if} \quad 0 < k \leq n-2, \\ 2(a_{n-2}^{(n)}) & \text{if} \quad k = n-1. \end{cases} \tag{2.2}$$

Using the recurrence relation (2.2), $g_n(x)$ is as follows:

$$\begin{aligned} g_1(x) &= 1 \\ g_2(x) &= 1 - 2x \\ g_3(x) &= 1 - 3x + 6x^2 \\ g_4(x) &= 1 - 4x + 10x^2 - x^3 \\ g_5(x) &= 1 - 5x + 15x^2 - 35x^3 + 70x^4 \\ &\vdots \qquad\qquad\qquad\qquad \vdots \end{aligned}$$

Then, $\varphi_{g_n}^{(pp)}$ has the following properties whose proofs can be found in [36].

- $\varphi_{g_n}^{(pp)}(x) + \varphi_{g_n}^{(pp)}(x-1) = 1$ for all $x \in [0, 1]$. Hence, $\{\varphi_{g_n}^{(pp)}(x-j) \mid j \in \mathbb{Z}\}$ is a partition of unity on $\mathbb{R}$.
- $\varphi_{g_n}^{(pp)}(x)$ is a $\mathcal{C}^{n-1}$ - function.
- The gradient of the scaled basis PU function is bounded as follows:

$$\frac{d}{dx}[\varphi_{g_n}^{(pp)}(\frac{x}{2\delta})] \leq \frac{C}{\delta}$$

Note that the constant C is ≤ 0.9 for $n \leq 3$

Using the basis PU function $\varphi_{g_n}^{(pp)}$, we construct a $\mathcal{C}^{n-1}$ - PU function with flat-top whose support is $[a-\delta, b+\delta]$ with $(a+\delta) < b-\delta$ as follows:

$$\Phi_{[a,b]}^{(\delta,n-1)}(x) = \begin{cases} \varphi_{g_n}^{L}(\frac{x-(a+\delta)}{2\delta}) \text{ if } x \in [a-\delta, a+\delta] \\ 1 \qquad \text{if } x \in [a+\delta, b-\delta] \\ \varphi_{g_n}^{R}(\frac{x-(b-\delta)}{2\delta}) \text{ if } x \in [b-\delta, b+\delta] \\ 0 \qquad \text{if } x \notin [a-\delta, b+\delta]. \end{cases} \tag{2.3}$$

Note that we assume that $\delta \leq \frac{b-a}{3}$ to make a PU function have a flat-top.

3. Formulations for Free Vibration and Buckling

3.1. **Governing Equations and Variational Formulation of Reissner-Mindlin Plates.** Following notations in the book [40], under the Kirchoff hypothesis but relaxing the normality condition, the displacement field of the first order theory can be expressed in the form

$$\begin{aligned} u(x,y,z,t) &= u_0(x,y,t) + z\phi_x(x,y,t), \\ v(x,y,z,t) &= v_0(x,y,t) + z\phi_y(x,y,t), \\ w(x,y,z,t) &= w_0(x,y,t). \end{aligned} \tag{3.1}$$

(u_0, v_0, w_0) denotes the displacements of a point on the plane $z = 0$ and ϕ_x and ϕ_y are the rotations of a transverse normal about the $y-$ and $x-$ axis as shown in Fig. 1, respectively

$$u_{,z} = \phi_x, \quad v_{,z} = \phi_y. \tag{3.2}$$

In the Reissner-Mindlin plate, bending and shear strains are only considered and they can be expressed in the vector form as

$$\{\varepsilon_b\} = \begin{Bmatrix} \phi_{x,x} \\ \phi_{y,y} \\ \phi_{x,y} + \phi_{y,x} \end{Bmatrix} \text{ and } \{\varepsilon_s\} = \begin{Bmatrix} w_{0,y} + \phi_y \\ w_{0,x} + \phi_x \end{Bmatrix}, \text{ respectively.} \tag{3.3}$$

The Euler-Lagrange equations of the Reissner-Mindlin plate can be derived by using the dynamic version of the principle of virtual displacements as follows:

$$\begin{aligned} M_{xx,x} + M_{xy,y} - Q_x &= \frac{\rho h^3}{12}\phi_{x,tt}, \\ M_{xy,x} + M_{yy,y} - Q_y &= \frac{\rho h^3}{12}\phi_{y,tt}, \\ Q_{x,x} + Q_{y,y} - \kappa w_0 + q &= \rho h w_{0,tt}, \end{aligned} \tag{3.4}$$

where M_{xx}, M_{yy}, and M_{xy} are bending moments and Q_x, Q_y are transverse force resultants, defined as follows:

$$\begin{Bmatrix} M_{xx} \\ M_{yy} \\ M_{xy} \end{Bmatrix} = \mathbf{D}\{\varepsilon_b\}, \quad \begin{Bmatrix} Q_y \\ Q_x \end{Bmatrix} = \mathbf{A}\{\varepsilon_s\}. \tag{3.5}$$

κ is the force constant, q is the transverse load applied at top and bottom in plate, h is the thickness of plate. In the relations (3.5), the bending stiffness coefficients $\mathbf{D}$ and the extensional stiffness coefficients $\mathbf{A}$ are defined as

$$\mathbf{D} = \begin{bmatrix} D_{11} & D_{12} & 0 \\ D_{12} & D_{22} & 0 \\ 0 & 0 & D_{66} \end{bmatrix}, \quad \mathbf{A} = \begin{bmatrix} A_{44} & 0 \\ 0 & A_{55} \end{bmatrix}, \tag{3.6}$$

where

$$\mathrm{D}_{11} = \frac{E_1 h^3}{12(1-\nu_{12}\nu_{21})}, \quad \mathrm{D}_{12} = \frac{\nu_{12} E_2 h^3}{12(1-\nu_{12}\nu_{21})}, \quad \mathrm{D}_{22} = \frac{E_2 h^3}{12(1-\nu_{12}\nu_{21})}$$
$$\mathrm{D}_{66} = \frac{G_{12} h^3}{12}, \qquad \mathrm{A}_{44} = G_{23} h, \qquad \mathrm{A}_{55} = G_{13} h$$

where E_i are Young's moduli, ν_{ij} are Poisson ratios, and G_{ij} is shear moduli.

For an isotropic plate, $E \equiv E_1 = E_2$ and $\nu \equiv \nu_{12} = \nu_{21}$ then (3.6) can be simplified as follows:

$$\mathbf{D} = \frac{Eh^3}{12(1-\nu^2)} \begin{bmatrix} 1 & \nu & 0 \\ \nu & 1 & 0 \\ 0 & 0 & \frac{(1-\nu)}{2} \end{bmatrix}, \quad \mathbf{A} = \frac{k_s E h}{2(1+\nu)} \begin{bmatrix} 1 & 0 \\ 0 & 1 \end{bmatrix}.$$

Using the relations (3.3), (3.5), and (3.6) and rewriting the Euler-Lagrange equations (3.4) in terms of the rotational displacements (3.2) , we obtain

$$\begin{aligned} D\big\{\phi_{x,xx} + \nu\phi_{y,yx} + \frac{(1-\nu)}{2}(\phi_{x,yy} + \phi_{y,xy})\big\} - Ah^{-2}(w_{0,x} + \phi_x) = 0, \\ D\big\{\phi_{y,yy} + \nu\phi_{x,xy} + \frac{(1-\nu)}{2}(\phi_{x,yx} + \phi_{y,xx})\big\} - Ah^{-2}(w_{0,y} + \phi_y) = 0, \\ -Ah^{-2}(w_{0,xx} + w_{0,yy} + \phi_{x,x} + \phi_{y,y}) = q, \end{aligned} \tag{3.7}$$

where D is the scaled bending modulus, $E/[12(1-\nu^2)]$, $A = Ek_s/2(1+\nu)$, and k_s is the transverse shear correction factor.

3.2. **Patchwise RPP Approximation Form.** Patchwise RPPM is a partition of unity finite element method (PUFEM) which uses RPP shape functions as local approximation functions. In this section, we construct local basis functions by using RPP shape functions and PU functions with flat-top constructed in [32].

Let $\Omega \subseteq \mathbb{R}^2$ be a polygonal domain, and let $\delta > 0$ be a real number. Let $\{\Omega_i \mid i = 1, 2, \cdots, N\}$ be a convex quadrangular partition of $E_\delta(\Omega)$, where $E_\delta(\Omega)$ is the δ-extension of Ω defined by

$$E_\delta(\Omega) = \bigcup_{\mathbf{x}\in\Omega_i} \left(\mathbf{x} + [-\delta, +\delta]^2\right).$$

Ω_i is called a patch. Note that the quadrangular patches Ω_i are allowed to be convex polygons, such as triangles, rectangles, non-rectangular quadrangles, pentagons, and so on.

For each $i = 1, 2, \cdots, N$, denote $X_i = \{\mathbf{x}_{i_j} \in \mathbb{R}^2 \mid j \in \Lambda_i\}$ as the particles associated with the patch Ω_i. Note that the particles do not need to be in Ω_i. Let $\{\psi_{i_j} \mid j \in \Lambda_i\}$ be the set of

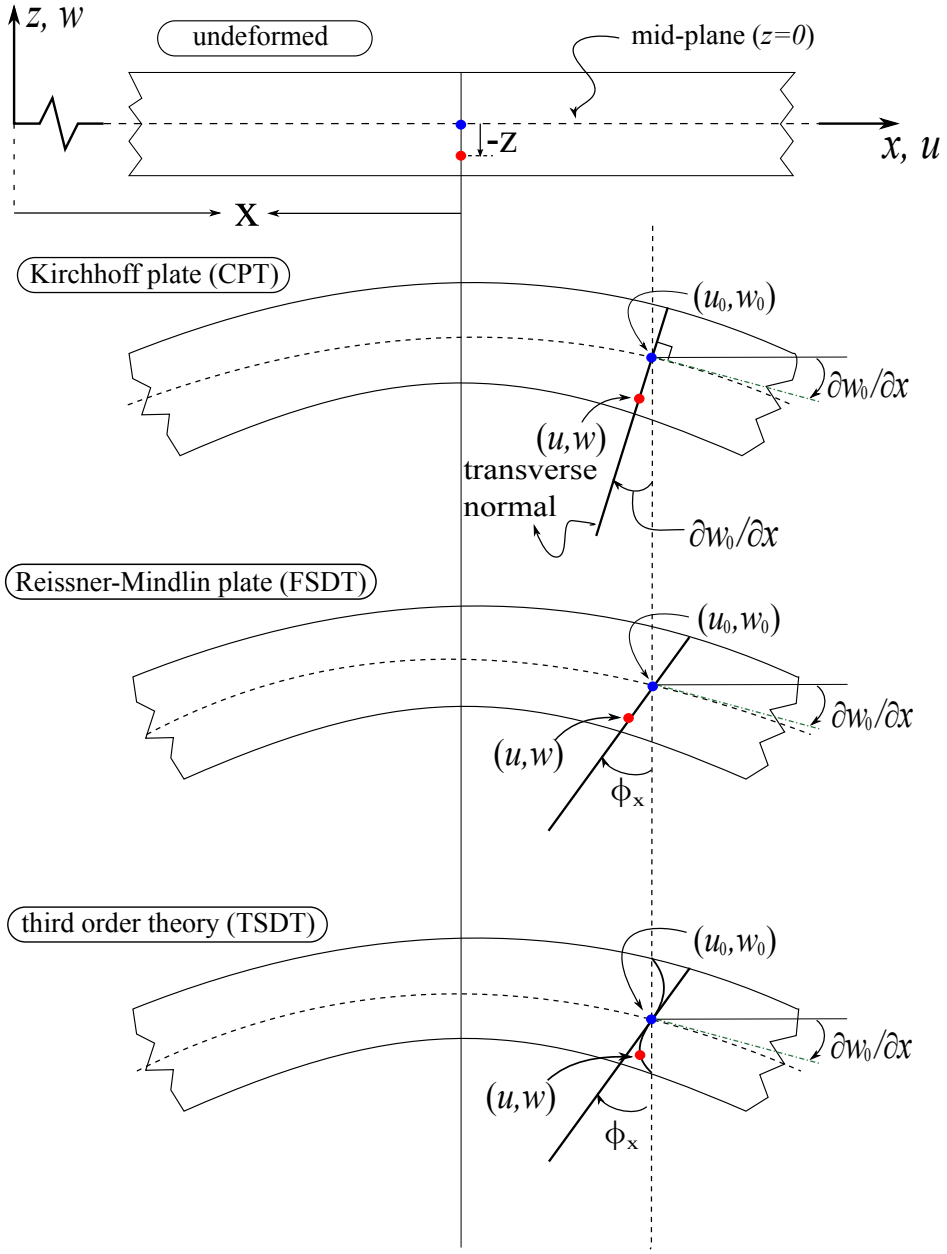

FIGURE 1. Deformation of a transverse normal according to Kirchoff (classical), Reissner-Mindlin (first order), and third order plate theories

$\mathcal{C}^r$-piecewise polynomial shape functions corresponding to the particles $\mathbf{x}_{i_j}$.
Now we define the local approximation of the displacement filed as follows:

$$\begin{aligned} w(\mathbf{x}) \approx w^{h_i}(\mathbf{x}) &= \sum_{j=1}^{n} \Psi_i(\mathbf{x})\psi_{i_j}(\mathbf{x})d_{ij}^{(1)}, \\ \phi_x(\mathbf{x}) \approx \phi_x^{h_i}(\mathbf{x}) &= \sum_{j=1}^{n} \Psi_i(\mathbf{x})\psi_{i_j}(\mathbf{x})d_{ij}^{(2)}, \\ \phi_y(\mathbf{x}) \approx \phi_y^{h_i}(\mathbf{x}) &= \sum_{j=1}^{n} \Psi_i(\mathbf{x})\psi_{i_j}(\mathbf{x})d_{ij}^{(3)}, \end{aligned} \tag{3.8}$$

for i-th patch Ω_i, where partition of unity with flat-top $\Psi_i(\mathbf{x})$ is the simple form of (2.3) in two-dimension.
Substituting (3.8) into the variational formulation obtained by Lagrange-Euler equations (3.7) with assumption of free vibration (i.e force vector is zero.), we can get the following matrix form

$$\mathbf{K}\mathbf{d} + \mathbf{M}\ddot{\mathbf{d}} = \mathbf{0}, \tag{3.9}$$

where

$$\mathbf{K} = \begin{bmatrix} [K_{11}] & [K_{12}] & [K_{13}] \\ [K_{12}] & [K_{22}] & [K_{23}] \\ [K_{13}] & [K_{23}] & [K_{33}] \end{bmatrix}, \ \mathbf{M} = \begin{bmatrix} [M_{11}] & 0 & 0 \\ 0 & [M_{22}] & 0 \\ 0 & 0 & [M_{33}] \end{bmatrix}, \text{ and } \mathbf{d} = \begin{Bmatrix} \{d^{(1)}\} \\ \{d^{(2)}\} \\ \{d^{(3)}\} \end{Bmatrix}. \tag{3.10}$$

Note that $\ddot{\mathbf{d}}$ is the accelerations and submatrices $[K_{ij}]$ and $[M_{ii}]$ are symmetric.
Assuming the harmonic motion we obtain the natural frequencies and the modes of vibration by solving the generalized eigenproblem [12]

$$\left(\mathbf{K} - \omega^2\mathbf{M}\right)\mathbf{X} = \mathbf{0},$$

where ω is the natural frequency and $\mathbf{X}$ the mode of vibration.

For buckling of plate models, the strain energy for in-plane pre-buckling stresses $\hat{\sigma}_x, \hat{\sigma}_y, \hat{\sigma}_{xy}$ without considering external forces is the following:

$$\begin{aligned} U = \frac{1}{2}\int_\Omega \varepsilon_b^T \mathbf{D}\varepsilon_b dxdy + \frac{1}{2}\int_\Omega \varepsilon_s^T \mathbf{A}\varepsilon_s dxdy + \frac{1}{2}\int_\Omega [w_{0,x}\ w_{0,y}]\hat{\sigma}^{\mathbf{0}} \begin{Bmatrix} w_{0,x} \\ w_{0,y} \end{Bmatrix} dxdy \\ + \frac{1}{2}\int_\Omega [\phi_{x,x}\ \phi_{x,y}]\hat{\sigma}^{\mathbf{0}} \begin{Bmatrix} \phi_{x,x} \\ \phi_{x,y} \end{Bmatrix} dxdy + \frac{1}{2}\int_\Omega [\phi_{y,x}\ \phi_{y,y}]\hat{\sigma}^{\mathbf{0}} \begin{Bmatrix} \phi_{y,x} \\ \phi_{y,y} \end{Bmatrix} dxdy, \end{aligned} \tag{3.11}$$

where

$$\hat{\sigma}^{\mathbf{0}} = \begin{bmatrix} \hat{\sigma}_x & \hat{\sigma}_{xy} \\ \hat{\sigma}_{xy} & \hat{\sigma}_{yy} \end{bmatrix}.$$

We can rewrite the strain energy (3.11) as the following matrix form

$$\mathbf{K}\mathbf{d} + \lambda\mathbf{G} = \mathbf{0}, \tag{3.12}$$

where $\mathbf{K}$ is the global stiffness matrix defined in (3.10),

$$\mathbf{G} = \begin{bmatrix} [G_{11}] & 0 & 0 \\ 0 & [G_{22}] & 0 \\ 0 & 0 & [G_{33}] \end{bmatrix},$$

which is called geometrical stiffness matrix and λ is a constant by which the in-plane loads must be multiplied to cause buckling. Thus the buckling loads can be found by solving the eigenproblem in (3.12).

4. Numerical Results

In order to show the effectiveness of the proposed meshfree method, we observe Reissner-Mindlin plates in bending, vibration, and buckling by means of the patchwise RPPM. Also, the comparison of our numerical results with other results are described in the following subsections.

4.1. **A Square Reissner-Mindlin Plate in Bending.** One can compare the approximate solutions obtained by the patchwise RPPM with conventional FEM using quadratic basis functions to see the effectiveness of the patchwise RPPM over FEM for the square Reissner-Mindlin plate in bending. To this end, we consider a simply-supported and clamped square plates (side $a = 1$) under uniform transverse pressure ($q = 1$), and thickness h. Other properties of the material are employed by ([12]). The non dimensional transverse displacement is set as

$$\hat{w} = w_{\text{max}} D/qa^4,$$

where D is the flexural rigidity, w_{max} is the absolute maximum value of transverse deflection and it occurs at center point in this problem. The numerical results in Table 1 show that RPPM is highly effective than conventional FEM even though we use less DOF for bending problem. Note that SSSS (CCCC) means that simply (clamped) supported boundary conditions are imposed along four sides of the square Reissner-Mindlin plate.

It verifies that the maximum transverse displacement w_{max} occurs at the center of the plate as shown in Fig. 2(a). Moreover, the rotational displacement ϕ_y is zero at the pair of two edges corresponding to the lines $y = 0$ and $y = 1$ because of the simply supported boundary conditions as shown in Fig. 2(b). In Fig. 2(c), twisting moment M_{xy} is shown in skew-symmetric form because of the simply supported boundary conditions.

4.2. **Reissner-Mindlin Plates in Free Vibration and Buckling.** In this subsection, we demonstrate the effectiveness of the proposed meshfree method (RPPM) in deal with thick plates of various thickness-to-edge ratios for free vibration and buckling. The ratios, RPP order, correction factors, non flat-top areas of PU functions that are used for numerical tests are as follows:

(1) we consider a square plate with side a with various thickness-to-width ratios and boundary conditions in Tables 2 through 7, and a rectangular plate with side a and length b with various length-to-width ratios as well as thickness-to-width ratios in Table 8

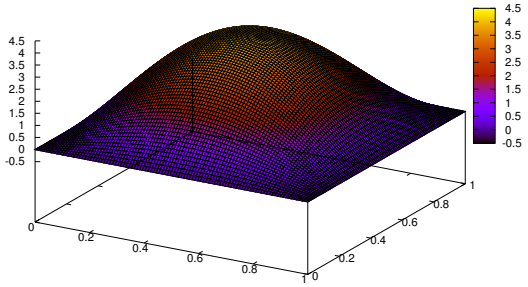

(a) ***Deformed shape of the plate along the displacement*** w

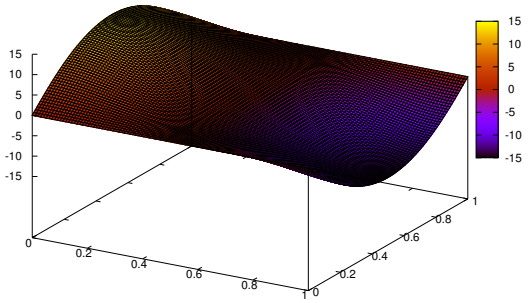

(b) ***Deformed shape of the plate along the displacement*** ϕ_y

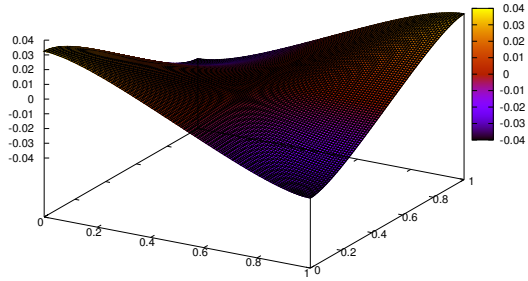

(c) ***Twisting moment*** M_{xy} ***of the plate***

FIGURE 2. (a) Maximum deflection of transverse displacement w occurs at the center of the plate (b) The rotational displacement ϕ_y is zero at the pair of two edges corresponding to the lines $y = 0$ and $y = 1$ because of the simply supported boundary conditions (c) It occurs in skew symmetric for the twisting moment because of simply supported bounday conditions

TABLE 1. non dimensional transverse displacement $\hat{w}$ of a square Reissner-Mindlin plate for two different ratios of a/h and boundary conditions under uniform transverse pressure ($q = 1$). $\hat{w}_k$ means RPP approximate solution with order of RPP k. Exact solutions, $\hat{w}_{\text{exact}}$'s are Navier solutions with 1000×1000 terms for each solutions [40].

a/h		10		20	
$\hat{w}$	DOF	SSSS	CCCC	SSSS	CCCC
$\hat{w}_2$	36	0.00404664880	0.000511155881	0.00355041532	0.00150427733
$\hat{w}_4$	100	0.00427089918	0.00150075015	0.00405976679	0.00125712238
$\hat{w}_6$	196	0.00427187070	0.00150406450	0.00406142190	0.00126486890
$\hat{w}_{\text{FEM}}$	961	0.004271	0.001503	0.004060	0.001264
$\hat{w}_{\text{exact}}$	∞	0.004271866	0.00150	0.004061413	0.001260

(2) we consider the Rayleigh-Ritz solutions as exact solutions [9, 19] in Tables 2, 3, and 8, and the Reissner-Mindlin solutions as exact solutions [17] in Tables 4 through 7
(3) Thickness-to-edge, h/a is set 0.1 in Tables 2, 4, and 6, and 0.01 in Tables 3, 5, and 7.
(4) we use the transverse shear correction factor, $k_s = 0.8601$ in Table 2, 0.833 in Tables 3 and 4, and 0.822 in Tables 5, 6 and 7.
(5) In Tables 2 through 7, we use RPP order 6, and we use RPP order 4 in Table 8. Note that particle shape functions are product of Lagrange interpolation polynomials corresponding to particles $x_0, \ldots, x_n$, n is an order of RPP shape functions.
(6) we use four patches with $\delta = 0.05$ in all of Tables as shown in Fig. 3(a).

The non-dimensional natural frequency (or fundamental frequency parameter) is given by

$$\bar{\omega} = \omega_{mn} a \sqrt{\rho/G},$$

where ρ is the material density, $G = E/2(1+\nu)$ is the shear modulus. m and n are the vibration half-waves in axes x and y, respectively.

In Tables 2 and 3, the clamped boundary conditions are imposed on all sides of the square Reissner-Mindlin plate (CCCC). With the clamped boundary conditions, two different thickness-to-edge ratios, 0.1 and 0.01 are considered. Also, the shear correction factor is taken as $k_s = 0.8601$. We compute the first thirteen modes of vibration for both the plates, and the non-dimensional natural frequencies computed by patchwise RPPM are compared with Rayleigh-Ritz solutions [8] for each plates in Tables 2 and 3. As you can see the modes from first to sixth in Tables 2 and 3, RPPM solutions are the closest approximations to the Rayleigh-Ritz solutions comparing with other solutions, classical Finite Element solutions using quadrilateral elements [12] and RKP solutions [22] as a comparative numerical result. Moreover, it is worth noticing that the proposed method use much less number of degrees of freedom than the others.

In Tables 4 and 5, fully simply supported (SSSS) Reissner-Mindlin square plates with different thickness-to-edge ratios, 0.1 and 0.01 are considered. Also the shear correction factor

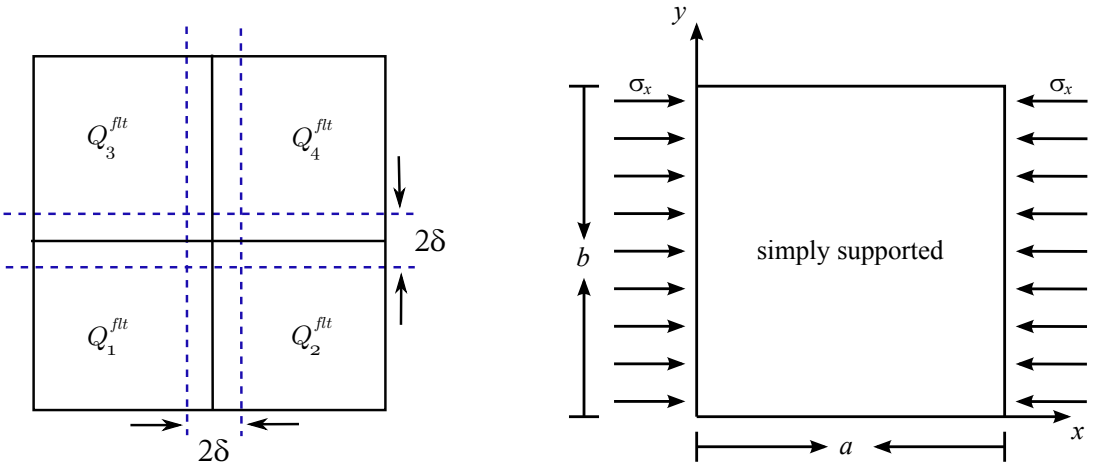

(a) ***Patches of plate*** **(b)** ***Rectangular plate subjected to in-plane compression loading***

FIGURE 3. (a) Partition of rectangular plate into four patches (b) Simply supported rectangular plates subjected to uniaxial compression

TABLE 2. Fundamental frequency parameters $\bar{\omega}_{mn}$ for a CCCC square Reissner-Mindlin plate with $h/a = 0.1$, $k_s = 0.8601$, $\nu = 0.3$

Method	FEM	RKPM	RPPM	Rayleigh-Ritz
DOF	441	289	196	·
Mode no.(m,n)				
1(1,1)	1.5955	1.5582	1.5910	1.594
2(2,1)	3.0662	3.0182	3.0390	3.039
3(1,2)	3.0662	3.0182	3.0390	3.039
4(2,2)	4.2924	4.1711	4.2627	4.265
5(3,1)	5.1232	5.1218	5.0255	5.035
6(1,3)	5.1730	5.1594	5.0731	5.078
7(3,2)	6.1587	6.0178	6.0808	·
8(2,3)	6.1587	6.0178	6.0808	·
9(4,1)	7.6554	7.5169	7.4204	·
10(1,4)	7.6554	7.5169	7.4204	·
11(3,3)	7.7703	7.7288	7.6814	·
12(4,2)	8.4555	8.3985	8.2671	·
13(2,4)	8.5378	8.3985	8.3426	·

TABLE 3. Fundamental frequency parameters $\bar{\omega}_{mn}$ for a CCCC square Reissner-Mindlin plate with $h/a = 0.01$, $k_s = 0.8601$, $\nu = 0.3$

Method	FEM	RKPM	RPPM	Rayleigh-Ritz
DOF	441	289	196	·
Mode no.(m,n)				
1(1,1)	0.175	0.1743	0.1753	0.1754
2(2,1)	0.3635	0.3576	0.3574	0.3576
3(1,2)	0.3635	0.3576	0.3574	0.3576
4(2,2)	0.5358	0.5240	0.5265	0.5274
5(3,1)	0.6634	0.6465	0.6401	0.6402
6(1,3)	0.6665	0.6505	0.6432	0.6402
7(3,2)	0.8266	0.8015	0.8020	·
8(2,3)	0.8266	0.8015	0.8020	·
9(4,1)	1.0875	1.0426	1.0317	·
10(1,4)	1.0875	1.0426	1.0317	·
11(3,3)	1.1049	1.0628	1.0681	·
12(4,2)	1.2392	1.1823	1.1820	·
13(2,4)	1.2446	1.1823	1.1872	·

TABLE 4. Fundamental frequency parameters $\bar{\omega}_{mn}$ for a SSSS square Reissner-Mindlin plate with $h/a = 0.1$, $k_s = 0.833$, $\nu = 0.3$

Method	FEM	RKPM	RPPM	3D solution	Mindlin solution
DOF	256	289	196	·	·
Mode no.(m,n)					
1(1,1)	0.9346	0.922	0.9302	0.932	0.930
2(2,1)	2.2545	2.205	2.2192	2.226	2.219
3(1,2)	2.2545	2.205	2.2192	2.226	2.219
4(2,2)	3.4592	3.377	3.4055	3.421	3.406
5(3,1)	4.3031	4.139	4.1493	4.171	4.149
6(1,3)	4.3031	4.139	4.1493	4.171	4.149
7(3,2)	5.3535	5.170	5.2054	5.239	5.206
8(2,3)	5.3535	5.170	5.2054	5.239	5.206
9(4,1)	6.9413	6.524	6.5237	·	6.520
10(1,4)	6.9413	6.524	6.5237	·	6.520
11(3,3)	7.0318	6.779	6.8338	6.889	6.834
12(4,2)	7.8261	7.416	7.4496	7.511	7.446
13(2,4)	7.8261	7.416	7.4496	7.511	7.446

TABLE 5. Fundamental frequency parameters $\bar{\omega}_{mn}$ for a SSSS square Reissner-Mindlin plate with $h/a = 0.01$, $k_s = 0.833$, $\nu = 0.3$

Method	FEM	RKPM	RPPM	Mindlin solution
DOF	441	289	196	·
Mode no.(m, n)				
1(1,1)	0.0965	0.0961	0.09628	0.09629
2(2,1)	0.2430	0.2419	0.24057	0.2406
3(1,2)	0.2430	0.2419	0.24057	0.2406
4(2,2)	0.3890	0.3860	0.38470	0.3848
5(3,1)	0.4928	0.4898	0.48077	0.4809
6(1,3)	0.4928	0.4898	0.48077	0.4809
7(3,2)	0.6380	0.6315	0.62463	0.6249
8(2,3)	0.6380	0.6315	0.62463	0.6249
9(4,1)	0.8550	0.8447	0.81910	0.8167
10(1,4)	0.8550	0.8447	0.81910	0.8167
11(3,3)	0.8857	0.8726	0.86410	0.8647
12(4,2)	0.9991	0.9822	0.96229	0.9605
13(2,4)	0.9991	0.9822	0.96229	0.9605

is taken as $k_s = 0.833$. In similar to Table 2 and 3, first thirteen modes of vibration have been calculated. Our RPPM solutions are compared with the 3-D elasticity solutions in Table 4 and analytical solutions given by Mindlin [17] in both Tables 4 and 5. The accuracy of our proposed method, patchwise RPPM is more agreeable than other two numerical results, FE solutions using quadrilateral elements [12] and RKP solutions [22] even though patchwise RPPM uses much less number of degrees of freedom than the others.

In Tables 6 and 7, the clamped and simply supported boundary conditions are imposed on each pairs of opposite sides in the square Reissner-Mindlin plates (SCSC) with the shear correction factor $k_s = 0.822$. RPPM solutions are compared with Mindlin solutions [17], and we can see that our RPPM solutions return better accuracy than the FE solutions [12].

In the buckling plate models, the non-dimensional buckling load intensity factor (or the critical buckling factor) is defined as

$$K_b = N_{cr} b^2/(\pi^2 D),$$

where b is the edge length of the plate as shown in Fig. 3(b), N_{cr} the critical buckling load, and D the flexural rigidity. In Table 8, we consider a rectangular Reissner-Mindlin plate with simply supported on each edge as shown in Fig. 3(b). Also, three different thickness-to-width ratios, $h/b = 0.05, 0.1, 0.2$, and five width-to-length ratios, $a/b = 0.5, 1, 1.5, 2, 2.5$ are considered. Our results by the proposed method are compared with those of the Ritz method

TABLE 6. Fundamental frequency parameters $\bar{\omega}_{mn}$ for a SCSC square Reissner-Mindlin plate with $h/a = 0.1$, $k_s = 0.822$, $\nu = 0.3$

Method	FEM	RPPM	Mindlin solution
DOF	256	196	·
$1(1,1)^{\text{Mode no.}(m,n)}$	1.2940	1.3001	1.302
2(2,1)	2.3971	2.3939	2.398
3(1,2)	2.9290	2.8845	2.888
4(2,2)	3.8394	3.8392	3.852
5(3,1)	4.3475	4.2314	4.237
6(1,3)	5.1354	4.9355	4.936
7(3,2)	5.5094	5.4575	·
8(2,3)	5.8974	5.7897	·
9(4,1)	6.9384	6.5584	·
10(1,4)	7.2939	7.2197	·
11(3,3)	7.7968	7.3062	·
12(4,2)	7.8516	7.5877	·
13(2,4)	8.4308	8.0734	·

TABLE 7. Fundamental frequency parameters $\bar{\omega}_{mn}$ for a SCSC square Reissner-Mindlin plate with $h/a = 0.01$, $k_s = 0.822$, $\nu = 0.3$

Method	FEM	RPPM	Mindlin solution
DOF	256	196	·
$1(1,1)^{\text{Mode no.}(m,n)}$	0.1424	0.1411	0.1411
2(2,1)	0.2710	0.2667	0.2668
3(1,2)	0.3484	0.3376	0.3377
4(2,2)	0.4722	0.4604	0.4608
5(3,1)	0.5191	0.4977	0.4979
6(1,3)	0.6710	0.6279	0.6279
7(3,2)	0.7080	0.6820	·
8(2,3)	0.7944	0.7524	·
9(4,1)	0.8988	0.8313	·
10(1,4)	1.0228	0.9706	·
11(3,3)	1.0758	1.0069	·
12(4,2)	1.1339	1.0190	·
13(2,4)	1.2570	1.1442	·

TABLE 8. The critical buckling factors, K_b, of simply supported rectangular plates with different length-to-width ratios a/b, and thickness-to-width ratios, t/b, subjected to uniaxial compression

Method		RKPM(Uniform particles)	RPPM	P-ver. Ritz
DOF		289	100	·
a/b	h/b			
0.5	0.05	6.0405	6.0344	6.0372
	0.1	5.3116	5.4604	5.4777
	0.2	3.7157	3.9428	3.9963
1	0.05	3.9293	3.9437	3.9444
	0.1	3.7270	3.7809	3.7865
	0.2	3.1471	3.2353	3.2637
1.5	0.05	4.2116	4.2567	4.2570
	0.1	3.8982	4.0179	4.0250
	0.2	3.1032	3.2705	3.3048
2	0.05	3.8657	3.9441	3.9444
	0.1	3.6797	3.7813	3.7865
	0.2	3.0783	3.2356	3.2637
2.5	0.05	3.9600	4.1213	4.0645
	0.1	3.7311	3.9038	3.8638
	0.2	3.0306	3.2276	3.2421

presented by Kitipornchai et al. [18] and RKPM with uniform particles [22], and details tabulated in Table 8. The results showed that the RPPM solutions are more accurate than the solutions obtained by RKPM with much less number of degrees of freedom.

5. CONCLUDING REMARK

In this paper, we proposed the patchwise Reproducing Polynomial Particle Method to compute the non-dimensional transverse displacement $\hat{w}$, natural frequency $\bar{\omega}_{mn}$, and buckling load intensity factor K_b. All numerical results have been compared with FE, RKP, and analytical solutions. They have shown us that RPP approximate solutions are highly effective than other numerical methods. Moreover, the proposed method has achieved accurate solutions with less computational work. These features make the RPPM appealing to obtaining the promising performance on thick plates which have various geometric configuration such as circular, skew or triangular plates. It will be considered in future work.

REFERENCES

[1] S. Atluri and S. Shen, *The Meshless Method*, Tech Science Press, 2002.

[2] I. Babŭska, U. Banerjee, and J.E. Osborn, *Survey of meshless and generalized finite element methods: A unified approach*, Acta Numerica, Cambridge Press, 2003, 1–125.

[3] I. Babŭska, U. Banerjee, and J.E. Osborn, *On the approximability and the selection of particle shape functions*, Numer. math, **96**, (2004), 601–640.

[4] T. Belytschko, D. Organ, and Y. Krongauz, *A coupled finite element-element-free Galerkin method*, Comput. Mech., **173(3)**, (1995), 186–195.

[5] C.W. Bert and M. Malik, *The differential quadrature method for irregular domains and application to plate vibration*, International Journal of Mechanical Sciences, **38(6)**, (1996), 589–606.

[6] S. Brenner and R. Scott, *The mathematical theory of finite element methods*, Springer, 1994.

[7] P.G. Ciarlet, *Basic error estimates for elliptic problems*, Handbook of Numerical Analysis Vol. II, North-Holland, 1991.

[8] D.J. Dawe and O.L. Roufaeil, *Rayleigh-Ritz vibration analysis of Mindlin plates*, Journal of Sound and Vibration, **45(1)**, (1980), 113–120.

[9] D.J. Dawe and O.L. Roufaeil, *Rayleigh-Ritz vibration analysis of Mindlin plates*, J. of Sound & Vibration, **69(3)**, (1980), 345–359.

[10] D.J. Dawe and S. Wang, *Spline finite strip analysis of the buckling and vibration of rectangular composite laminated plates*, International Journal of Mechanical Sciences, **37(6)**, (1995), 589–606.

[11] Duarte C.A. and J.T. Oden, *An hp adaptive method using clouds*, Computer methods in App. Mech. Engrg, **139**, (1996), 237-262.

[12] A.J.M. Ferreira, *MatLab Codes for Finite Element Analysis (Solids and Structures)*, Springer, 2009.

[13] M. Griebel and M.A. Schweitzer, *Meshfree Methods for partial Differential Equations I*, Lect. Notes in Compu. Science and Engr., Springer, **57**, 2003.

[14] M. Griebel and M.A. Schweitzer, *Meshfree Methods for partial Differential Equations II*, Lect. Notes in Compu. Science and Engr., Springer, **43**, 2005.

[15] M. Griebel and M.A. Schweitzer, *Meshfree Methods for partial Differential Equations III*, Lect. Notes in Compu. Science and Engr., Springer, **26**, 2007.

[16] W. Han and X. Meng, *Error analysis of reproducing kernel particle method*, Comput. Meth. Appl. Mech. Engrg., **190**, (2001), 6157–6181.

[17] E. Hinton, *Numerical methods and software for dynamic analysis of plates and shells*, Pineridge Press, Swansea, U.K., 1988.

[18] S. Kitipornchai, Y. Xiang, C.M. Wang, and K.M. Liew, *Buckling of thick skew plates*, International Journal for Numerical Methods in Engineering, **36**, (1993), 1299–1310.

[19] K.M. Liew, C.M. Wang, Y. Xiang, and S. Kitipornchai, *Vibration of Mindlin Plates*, Elsevier, Amsterdam, 1998.

[20] S. Li and W.K. Liu, *Meshfree Particle Methods*, Springer-Verlag, 2004.

[21] S. Li, Lu, H., W. Han., W.K. Liu, and D.C. Simkins Jr., *Reproducing Kernel Element Method: Part II. Globally Conforming I^m/C^n hierarchies*, Computer Methods in App. Mech. and Engrg, **193**, (2004), 953–987.

[22] K.M. Liew, J. Wang, T.Y. Ng, and M.J. Tan, *Free vibration and buckling analyses of shear-deformable plates based on FSDT meshfree method*, J. of Sound & Vibration, **276**, (2004), 997–1017.

[23] K.M. Liew, Y. Xiang, and S. Kitipornchai, *Research on thick plate vibration: a literature survey*, Journal of Sound and Vibration, **180(1)**, (1995), 163–176.

[24] G.R. Liu and X.L. Chen, *A mesh-free method for static and free vibration analysises of thin plates of complicated shape*, J. Sound and Vibration, **241(5)**, (2001), 839–853.

[25] W.K. Liu, W. Han, H. Lu, Li, S., and J. Cao, *Reproducing Kernel Element Method: Part I. Theoretical formulation*, Computer Methods in App. Mech. and Engrg, **193**, (2004), 933–951.

[26] W.K. Liu, S. Jun, and Y.F. Zhang, *Reproducing Kernel Particle Methods*, International Journal for Numerical Methods in Fluids, **20**, (1995), 1081–1106.
[27] W.K. Liu, S. Li, and T. Belytschko, *Moving Least Square Reproducing Kernel Method Part I: Methodology and Convergence*, Computer Methods in Applied Mechanics and Engineering, **143**, (1997), 422–453.
[28] W.K. Liu, S. Jun Liu, S. Li, J. Adee, and T. Belytschko, *Reproducing Kernel Particle Methods for Structural Dynamics*, International Journal for Numerical Methods in Engineering, **38**, (1995), 1655–1679.
[29] V.V. Meleshko, *Bending of an Elastic rectangular clamped plate: Exact versus Engineering solutions*, Journal of Elasticity, **48**, (1997), 1–50.
[30] A.K. Noor, *Free vibrations of multilayered composite plates*, American Institute of Aeronautics and Astronautics Journal, **11(7)**, (1973), 1038–1039.
[31] B. Szabó and I. Babŭska, *Finite element analysis*, John Wiley, 1991.
[32] H.-S. Oh and J. W. Jeong, *reproducing Polynomial (Singularity) Particle Methods and Adaptive Meshless Methods for Two-Dimensional Elliptic Boundary Value Problems*, Comput. Methods Appl. Mech. Engrg., **198**, (2009), 933–946.
[33] H.-S. Oh and J.W. Jeong, *Almost Everywhere Partition of Unity to deal with Essential boundary Conditions in Meshless Methods*, Compt. Meth. Appl. Mech. Eng., **198**, (2009), 3299–3312.
[34] H.-S. Oh, J.W. Jeong, and W.T. Hong, *The generalized product partition of unity for the meshless methods*, Journal of Comp. Phy., **229**, (2010), 1600–1620.
[35] H.-S. Oh, J.W. Jeong and J. G. Kim, *The Reproducing Singularity Particle Shape function for problems containing singularities*, Comput Mech, **41**, (2007), 135–157.
[36] H.-S. Oh, J. G. Kim, and W.T. Hong, *The Piecewise Polynomial Partition of Unity Shape Functions for the Generalized Finite Element Methods*, Comput. Methods Appl. Mech. Engrg., **197**, (2008), 3702–3711.
[37] H.-S. Oh, J.G. Kim, and J.W. Jeong, *The Closed Form Reproducing Polynomial Particle Shape Functions for Meshfree Particle Methods*, Comput. Methods Appl. Mech. Engrg., **196**, (2007), 3435–3461.
[38] H.-S. Oh, J.G. Kim, and J.W. Jeong, *The smooth piecewise polynomial particle shape functions corresponding to patchwise non-uniformly spaced particles for meshfree particles methods*, Computational Mechanics, **40**, (2007), 569–594.
[39] J.N. Reddy, *A review of refined theories of laminated composite plates*, The Shock and Vibration Digest, **22(7)**, (1990), 3–17.
[40] J.N. Reddy, *Theory and Analysis of Elastic Plates, Second Edition*, CRC Press, 2006.
[41] J.N. Reddy and A.A. Khdeir, *Buckling and vibration of laminated composite plates using various plate theories*, American Institute of Aeronautics and Astronautics Journal, **27(12)**, (1989), 1808–1817.
[42] T. Stroubolis, K. Copps, and I. Babŭska, *Generalized Finite Element method*, Comput. Methods Appl. Mech. Engrg., **190**, (2001), 4081–4193.
[43] T. Stroubolis, L. Zhang, and I. Babŭska, *Generalized Finite Element method using mesh-based handbooks: application to problems in domains with many voids*, Comput. Methods Appl. Mech. Engrg., **192**,, (2003), 3109–3161.
[44] A. Tessler, E. Saether, and T. Tsui, *Vibration of thick laminated composite plates*, Journal of Sound and Vibration, **179(3)**, (1995), 475–498.
[45] H. Zeng and C.W. Bert, *A differential quadrature analysis of vibration for rectangular stiffened plates*, Journal of Sound and Vibration, **241(2)**, (2001), 247–252.